OIKOS

Research

The dynamics of open populations: integration of top–down, bottom–up and supply–side influences on intertidal oysters

David L. Kimbro, J. Wilson White and Edwin D. Grosholz

D. L. Kimbro (https://orcid.org/0000-0003-4711-3531) (d.kimbro@northeastern.edu), Dept of Marine and Environmental Science, Northeastern Univ., Nahant, MA 01908, USA. – J. W. White (https://orcid.org/0000-0003-3242-2454), Dept of Fisheries and Wildlife, Coastal Oregon Marine Experiment Station, Oregon State Univ., Newport, OR, USA. – E. D. Grosholz (https://orcid.org/0000-0003-0327-0367), Dept of Environmental Science and Policy, Univ. of California Davis, Davis, CA, USA.

Oikos
00: 1–12, 2018
doi: 10.1111/oik.05892

Subject Editor: Dustin Marshall
Editor-in-Chief: Gerlinde De Deyn
Accepted 13 October 2018

Most communities are structured not by a single process but by some combination of top–down, bottom–up and supply–side (i.e. juvenile recruitment) factors. However, establishing how multiple processes interact remains a fundamental challenge. For example, the recruitment, growth, and mortality of estuarine species can vary along the steep and numerous environmental and biological gradients typical of these habitats, but the relative importance of those gradients is generally unknown. We took a novel approach to this question by coupling long-term field observations of the Olympia oyster *Ostrea lurida* in a central California estuary with a state–space integral projection model. This approach revealed that the most parsimonious description of oyster population dynamics involved spatial variation in growth and adult mortality – but not juvenile mortality – as well as spatiotemporal variation in recruitment. These patterns match the available short-term estimates of each of those processes from field studies, and reveal a synthetic view of oyster population dynamics. Larval recruitment has an interannual 'boom and bust' pattern, and during good recruitment years most larvae settle in the inner bay where water residence time is highest. Adult oyster mortality is also highest in the inner bay, where several invasive predators are abundant and lowest in the mid-bay, where oyster growth is greatest (due to bottom–up factors), likely leading to a size refuge from native predators. Surprisingly, juvenile mortality was constant across the bay, possibly because of a lack of size refuge from native and invasive predators. Our research approach represents an important advance in disentangling the contributions of spatio–temporal variation in top–down, bottom–up and supply–side forces to the dynamics of populations with open recruitment.

Keywords: benthic–pelagic coupling, invasion, Olympia oyster, physical forcing, predation, primary production, recruitment, state–space model

Introduction

An important debate in ecology concerns whether populations are controlled more from the 'top–down' by consumers (i.e. predation or herbivory) or from the 'bottom–up' by resource supply (i.e. nutrient availability, primary productivity or prey availability;

NORDIC SOCIETY OIKOS

www.oikosjournal.org

Hairston et al. 1960, Carpenter et al. 1985, Menge 1992, Polishchuk et al. 2012). This debate becomes more complicated when population renewal rates fluctuate with variable recruitment of dispersing propagules (e.g. planktonic larvae or wind-dispersed seeds). For a prey population that is relatively 'open' due to propagule dispersal, it has been posited that top–down control becomes important only when propagule supply yields prey abundances high enough to support predation by higher trophic levels (Gaines and Roughgarden 1985, Lewin 1986, Polis and Hurd 1996, Menge 2000). Similarly, bottom–up effects on growth and survival only become detectable when propagules are actually delivered to a habitat patch. Thus, distinguishing the effects of top–down versus bottom–up control requires simultaneously considering the 'supply–side' influence of recruitment (Lewin 1986).

As with most ecological paradigms, the top–down/bottom–up/supply–side conceptual approach is useful not as an absolute set of categories, but as a framework to characterize different dynamics among communities. For instance, differences in the supply of larvae (supply–side) can alter the importance of predation (top–down control) on barnacles over the spatial scale of only tens of meters (Gaines and Roughgarden 1985). Meanwhile, large-scale productivity differences in vegetation and small game prey (grouse, hare; bottom–up) can shift the importance of top–down predation on mesopredator foxes by wolf and lynx across bioclimatic regions of Scandinavia separated by hundreds of kilometers (Elmhagen and Rushton 2007). Further advances in this field depend on both an integration of top–down, bottom–up and supply–side controls into one framework and the application of this framework to understand the spatial and temporal scales over which the relative importance of one control or interplay of all three vary.

The balance among bottom–up, top–down and supply–side factors has often been investigated with the comparative-experimental approach (CEA), which involves combining local-scale experiments on species interactions with monitoring of important biotic and abiotic factors across large spatial scales (Leonard et al. 1998, Menge et al. 2003). As an example, Orrock et al. (2014) used a standardized experiment replicated across temperate North America to examine whether climate conditions affected granivore predation on oat seeds *Avena sativa*. They found that the rate of seed loss from experimental depots was driven by continent-scale variation in evapotranspiration. While this and other factorial models can productively test whether single factors or combinations of factors differ statistically over space and time (Stiling and Rossi 1997), experimental approaches cannot necessarily reveal whether spatial or temporal variation in those factors is ecologically significant in terms of generating spatiotemporal patterns in population or community dynamics. For example, experiments and field observations demonstrated that red sea urchins *Mesocentrotus franciscanus* have a refuge from predation at small sizes (due to aggregation under adult spine canopies) and large sizes (due to predator gape limitation). These patterns were thought to explain the bimodal size distribution of some urchin populations (Tegner and Dayton 1981, Tegner and Levin 1983). However, a size-structured population model revealed that the bimodal distribution could be produced by the upper size refuge alone; the juvenile size refuge was not responsible for the lower mode (Botsford et al. 1994). Furthermore, if the influences of supply–side, top–down and bottom–up controls fluctuate over time, then short-term experiments may not detect the correct set of factors that shaped the density or age structure of a focal prey population (Hastings 2010).

As a way forward, we combined the traditional CEA with a population modeling approach to investigate the dynamics of the Olympia oyster *Ostrea lurida*, a non-harvested intertidal bivalve that is a foundation species in Pacific coast estuaries of North America (Kimbro and Grosholz 2006, Pritchard et al. 2015). We used data from eight years of CEA research on this species in a California (USA) estuary, quantifying several factors affecting the growth and mortality of adult and juvenile oysters: a predatory invasive snail (*Urosalpinx cinerea*, top–down control), meso-scale oceanographic processes that locally influence the abundance of phytoplankton on which oysters feed (bottom–up control), and oyster larval recruitment (supply–side; Kimbro et al. 2009a, b). Although this CEA work was comprehensive in identifying spatiotemporal patterns in all of the major factors affecting oyster populations, it did not provide a complete understanding of oyster population dynamics because each factor was examined in isolation and for only a few annual cohorts (Kimbro et al. 2009a,b).

Here, we developed a better understanding of how these factors interact over space and time by using state–space population models fit to long-term observations of population density and size distribution. We developed a suite of candidate models representing all possible combinations of spatial and temporal variation in top–down, bottom–up and supply–side factors identified by prior research, then used information-theoretic criteria to identify the model that best explained the observed spatiotemporal patterns in the observed data. This approach identified the combination of factors that interact to structure oyster population dynamics in the estuary, and also assessed the relative importance of variability in those factors over space and time. Our approach affords a comprehensive synthesis of short-term experimental results and long-term monitoring data to understand population patterns.

Methods

Study system

We investigated Olympia oyster populations in Tomales Bay, California, a 20 × 1 km basin, where oysters are restricted to intertidal habitats (Hearn and Largier 1997, Kimbro et al. 2009a). Physical conditions in the bay lead to opposing gradients in bottom–up, supply–side and top–down factors (Fig. 1A), as we now detail.

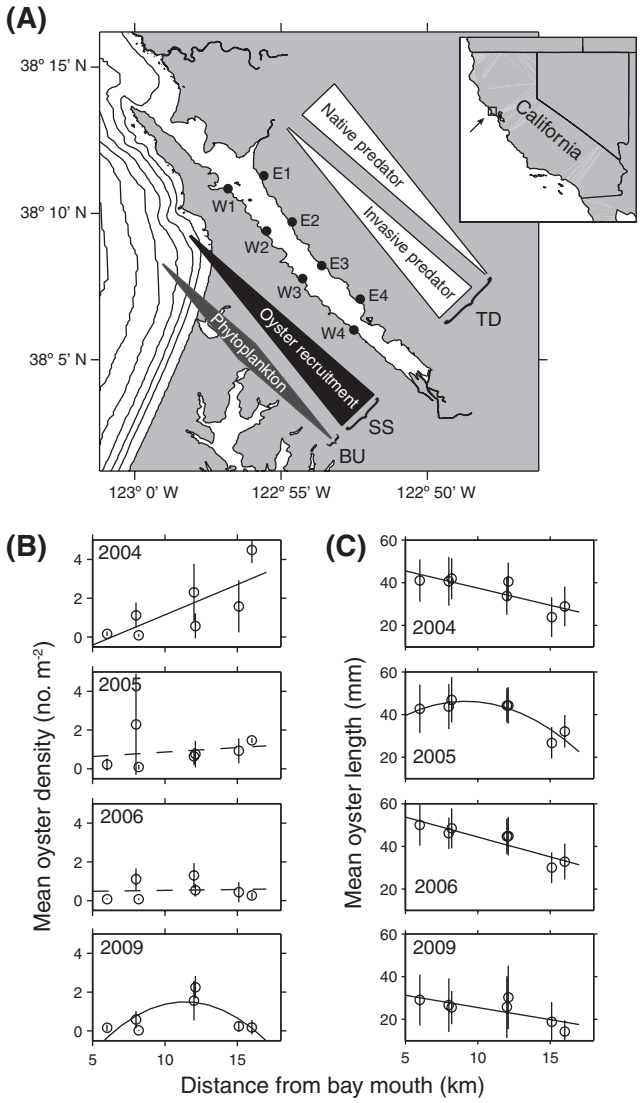

Figure 1. (A) Schematic of study sites in Tomales Bay, CA and gradients of top–down (TD), bottom–up (BU), and supply–side (SS) factors. (B) Population density and (C) mean oyster size as a function of distance from the mouth of the bay in each of four study years. Solid curves depict statistically significant relationships; dashed curves are not significant. Error bars indicate 1 SD. Contour lines are 10 m.

In the dry season (May–October), intense coastal upwelling and low freshwater inflow produce opposing gradients in water residence times (highest in the inner bay) and nutrient concentrations (highest in outer bay). Together these opposing gradients yield maximum phytoplankton productivity in the middle bay (Fig. 1A; Largier et al. 1997, Kimbro et al. 2009b; for details, Supplementary material Appendix 1). Oysters are suspension feeders on phytoplankton, so this spatial gradient in productivity generates a corresponding spatial pattern in oyster growth (faster growth in the mid-bay; see gray diamond labeled 'phytoplankton' that peaks in mid bay of Fig. 1A). This is the primary bottom–up control on oyster populations that was consistently detected in field experiments (Kimbro et al. 2009b).

During the dry season, the lack of inflow from the watershed produces an increasing gradient of residence time from the mouth to the head of the estuary (Hearn and Largier 1997). This gradient is expected to promote a larval retention zone (sensu Wing et al. 1998) with greater accumulation of planktonic oyster larvae in the inner bay. Consequently, we predicted and tested that oyster recruitment (the supply–side factor) should increase from the outer to the inner bay (see the black wedge labeled 'oyster recruitment' increasing from outer to inner bay in Fig. 1A).

Top–down control on oysters by predators also varies spatially. During rainy winters, freshwater stream input into the inner bay causes salinity to decrease from the mouth to the head of the bay (Supplementary material Appendix 1 Fig. A1). Although extremely low salinities can kill oysters (Kimbro et al. 2009a, Cheng et al. 2017), a more important effect of this spatial gradient in environmental stress is that it restricts native oyster predators (primarily the rock crabs, *Cancer antennarius* and *C. productus*, and angular unicorn snail, *Acanthinucella spirata*) to the outer bay (see wedge labeled 'native predators' declining from outer to inner bay in Fig. 1A; Kimbro et al. 2009a). But a different predator assemblage appears to be tolerant of low-salinity inner-bay conditions: the non-native oyster drill *Urosalpinx cinerea* and the non-native European green crab *Carcinus maenas*; an additional non-native snail *Ocinebrellus inornatus* recently invaded Tomales Bay, but it was not present during our study. Neither non-native species is found elsewhere in the bay because of predation by and fear of native crabs (Jensen et al. 2007, Kimbro et al. 2009a; see the white wedge labeled 'invasive predators' declining from inner to outer bay in Fig. 1A). This spatial distribution of predators causes high adult oyster mortality in the inner bay (from invasive drills) and lower mortality in the middle (and likely outer) bay, where we suspect native crabs suppress predation by native gastropods (Kimbro et al. 2009a). We predicted that the same suite of predator dynamics would yield a similar spatial pattern for juvenile oyster mortality.

We collected all data for this study at eight study sites in Tomales Bay, which were arrayed as four east–west pairs (Fig. 1A, Table 1). The four pairs were spaced evenly along the axis of the bay at increasing distance from the mouth with the two sites closest to the estuary mouth receiving the greatest ocean influence (E1, W1) and the two sites closest to the estuary head receiving the greatest influence from a freshwater creek (E4, W4). As a result, the sites naturally grouped into three regions of the bay, defined by salinity, temperature and the biological community (Hearn and Largier 1997, Kimbro et al. 2009a,b): outer bay (E1, W1), mid-bay (E2–3, W2–3), and inner bay (E4, W4; Fig. 1A).

Modeling approach

Our overall approach was to fit population models to oyster size and abundance data collected at each of the field sites. We fit a suite of 216 different models, each representing a hypothesis about the combination of spatial and temporal patterns of bottom–up, top–down, and supply–side factors.

We then used model selection to identify the pattern that most parsimoniously fit the observed data. We first describe the collection of field data on oyster size and abundance and long-term growth, which were used to parameterize and fit the models. We then describe our model and model selection methods in detail. Finally, we describe the collection of two field datasets used for model validation: larval recruitment monitoring and a short-term predation experiment. The types of field data collected at each site and year and the role of each data type are described in Table 1.

Field data for model parameterization and fitting

Adult size and abundance surveys

We conducted annual surveys of oyster population density and size structure at each site in 2004–2006 and 2009 (Table 1). Sampling procedures are described in Kimbro et al. (2009a) and Supplementary material Appendix 2. The state-space oyster population model was fit to these data. Because oysters were never observed at site W1, we excluded this site from the empirical analyses and from the modeling analysis.

Site-specific growth trajectories of oysters

Kimbro et al. (2009b) described a consistent mid-bay peak in phytoplankton during the summer months and used multiple field experiments to establish that phytoplankton concentration is the primary control of juvenile oyster growth. Using laboratory reared juveniles out-planted in the field in 2006 and 2007, Kimbro et al. (2009b) found faster growth in the mid-bay than in the other two regions in both study years. In the present study, we examined previously unpublished data from a similar experiment in 2005, which was monitored for an additional 27 months (30 months total), to determine whether this bottom–up control due to persistent spatial variation in phytoplankton density produces spatial variation in growth trajectories over longer time periods. This allowed us to obtain site-specific growth trajectories for oysters of the same age and size over 30 months (experimental details and raw data over the entire 30-month study are presented in Supplementary material Appendix 3). Within the state-space population model, these site-specific, size-at-age relationships were used to describe bottom–up control due to persistent spatial variation in phytoplankton density.

State-space population model

To determine what combination of top–down, bottom–up and supply–side factors structured oyster populations in Tomales Bay, we created a state–space model of oyster population dynamics. Although state–space models are prominent in electrical engineering (Kalman 1960) and have a history of application in ecology (de Valpine and Hastings 2002, Dennis et al. 2006, Patterson et al. 2008), they are not a widely used tool in population dynamics. A state–space model has two components: an underlying process model representing the 'true' system dynamics, and an observation model that represents the data human observers collect about the system. The process model can include both deterministic processes (e.g. a mortality rate that specifies how many individuals are in the population at time $t+1$, given the abundance at time t) and process error (e.g. stochastic variability in the mortality rate). Additionally, it can incorporate measurement error in the observation model. A state–space model operates by initially predicting the system state at time $t+1$ (based on the state at time t or possibly at different lag times into the past), comparing that prediction to the observed data at time $t+1$, and then updating ('filtering') the prediction for $t+1$ to better match the observation, given the estimated rates of process and measurement error. Such a model has the advantage of capturing key realities of an ecological system (e.g. a population with variable dynamics that is observed imperfectly). Furthermore, if properly implemented, a state–space model can estimate both the process error and the measurement error, providing a better representation of the 'true' population state and consequently the underlying dynamics of the process model. Thus state–space approaches are a powerful tool for fitting models to noisy ecological time series.

Because we were fitting the model to size-structured survey data, we used a size-based integral projection model (IPM; Easterling et al. 2000, Ellner et al. 2016) as the deterministic process model, and used a particle filter (Knape and de Valpine 2012) to estimate process variability in the system. Integral projection models are similar to size- or stage-structured models (Caswell 2001) except that rather than dividing a population size distribution into a number of discrete bins (which requires choosing arbitrary size divisions and can lead to artifacts because within-bin dynamics are ignored), the state variable is a continuous size distribution.

Table 1. Summary of sampling effort for empirical data collection, indicating the individual sites at which each data type was collected and the year of collection (• indicates all sites were sampled). The role of each data type (model parameterization, model validation, or data to which model was fit) is also indicated.

Data type	Role	2002	2003	2004	2005	2006	2007	2008	2009	2010	2011
Surveys											
Larval recruitment	validation	E4, W4	•	•	•	•	•	•			
Adult size and abundance	data for fitting			•	•	•			•		
Experiments											
Growth trajectory	parameterization				•	•	•				
Post-settlement mortality	validation										E1, W2, W3, W4, and 3 sites between W3 and W4

Consequently, transitions between sizes (e.g. growth, mortality) can be represented by continuous functions of size. Thus, such models are naturally suited to describe time series of size–abundance data and populations with size-dependent growth and mortality rates (White et al. 2016).

Our modeling framework and fitting methods were based on the state–space IPM developed by White et al. (2016), who described the method and showed that it could accurately estimate unknown demographic parameters when fitted to time series data. The model was linear and operated in discrete time, with an annual time step corresponding to the annual population surveys of oysters in Tomales Bay. We assumed that our observations of the oyster population included measurement error, and that there was also year-to-year stochastic variability in demographic rates due to process error.

The process model (the IPM) described the abundance of oysters of size x at time $t+1$ and site i, $N_i(x,i,t+1)$, as a function of survival, larval recruitment, and random variability (process error):

$$N(x,i,t+1) = \int_{\Omega} K(x,y,i,t)\,N(y,i,t+1)\,dy + R(i,t)\,\rho(x) + \upsilon(x,i,t). \quad (1)$$

The first term on the right-hand side (RHS) of this equation is the typical IPM formulation. The 'kernel', $K(x,y,i,t)$, describes the probability density of an oyster of size y in time t surviving and growing to size x in one time step. Both K and N are continuous distributions, and their product is integrated with respect to size over the entire range of possible oyster sizes, Ω. Within K, the survival rate was constant with size, except for the size range corresponding to new (age-0) recruits, which had a separate survival rate parameter. The second term on the RHS describes larval recruitment as the product of the total number of recruits $R(i,t)$ and the recruit size distribution $\rho(x)$. This corresponds to an annual input of recruits from an external source. This is because the relative contribution of larvae settling to each site from sources inside and outside Tomales Bay is unknown (though the supply from external sources is likely low), and the rate of larval supply to locations within the bay depends heavily on physical factors (e.g. residence time). Thus, we focused on factors that alter the magnitude of recruitment events rather than attempting to represent patterns of demographic connectivity in the larval stage. Consequently, there were no terms for fecundity or reproduction in the kernel, K. Finally, the third term on the RHS represents process error affecting the abundance of oysters of size x. Note that all three RHS terms can vary among sites and over time; the manner in which they varied depended on the particular top–down/bottom–up/supply–side model being used. Additional details of the model formulation are in Supplementary material Appendix 4.

For two reasons, the model did not include density-dependence. First, oyster densities are generally low in this system (mean <60% space occupancy on rocks in oyster habitat within the bay; Kimbro unpubl.), suggesting that density effects may be minimal relative to other rocky intertidal systems. Second, most density-dependence would be expected to occur soon after larval settlement, when densities are highest. However, in our model we estimated recruitment $R(i,t)$, which was based only on survey observations of juvenile size classes in site i, year t. In addition, these surveys occurred several months after the autumn larval settlement season. Thus, any density-dependence would likely have occurred prior to our first observation of juvenile oysters. Fortunately, our experimental estimation of post-settlement oyster mortality allowed us to determine whether there was any spatial variation in mortality rates during the time between settlement and survey. If density-dependent mortality occurred during the juvenile–adult transition or in the adult stage (e.g. due to crowding), then it could be accommodated for by higher estimates of juvenile or adult mortality rates in years following high recruitment events. Thus, our approach accommodated the effects of density-dependence without the additional difficulty of modeling nonlinear processes explicitly.

To fit the model to survey data for a particular site i, we simulated a deterministic version of the model (using time-averaged values for K and R and no process error and starting at an arbitrary initial size distribution), for 50 years to obtain the deterministic stable size distribution. We then initialized the state–space model with the stable size distribution for the year 2000 and ran it forward 10 years to 2009. For the four years with field data (2004–2006, 2009) we calculated the likelihood of the model given the data by comparing model predictions, $N(x,i,t)$ to the size–abundance data. The data were counts, so we calculated the likelihood using a Poisson distribution with expectation $N(x,i,t)$. Because the variance of a Poisson distribution is equal to the mean, there was no need for a separate measurement error parameter. After each model–data comparison, the state–space model accounted for process and measurement error by updating its estimate of $N(x,i,t)$ using a particle filter (Knape and de Valpine 2012, White et al. 2016). Each of the candidate top–down/bottom–up/supply–side models contained unknown parameters, which we estimated by fitting the model using a Bayesian Markov chain – Monte Carlo procedure (White et al. 2016; Supplementary material Appendix 4 for detailed methods).

Model selection

Our model included parameters describing the three major factors assumed to structure oyster population dynamics: bottom–up (growth, due to phytoplankton density), supply–side (recruitment), and top–down (mortality). Each of these factors could vary spatially and temporally. Based on prior research (Fig. 1A), we expected spatial variation in these factors to either follow a linear gradient (e.g. increasing or decreasing from outer bay to inner bay) or to have a maximum (or minimum) in the mid-bay, decreasing (or increasing) in either direction. For juvenile mortality, adult mortality, and recruitment, we considered models in which those demographic rates were 1) constant across sites, 2) varied linearly,

as a function of the distance of each site from the mouth of the bay, or 3) varied nonlinearly, as a quadratic function of the distance from the mouth of the bay. The parameters of those functions (intercept, slope, and, for the quadratic, the location of the mode) were estimated by the model. Temporal variation was added by allowing the intercept of each of those three functions (constant, linear, quadratic) to vary annually. That is, the spatial gradient was assumed to be constant over time, but the overall magnitude of survival or recruitment varied (Supplementary material Appendix 4 for details).

For growth, we considered scenarios in which each site had a unique growth rate (based on our site-specific data, and representing the bottom–up influence of phytoplankton availability) or in which all sites had the same growth rate (an average across data from all sites). We did not consider temporal variability in growth because prior analysis showed that the among-site spatial patterns were consistent across years (Kimbro et al. 2009b).

To determine which combination of spatial gradients and temporal variability in demographic rates best explained the observed population dynamics, we fit a suite of 216 candidate models representing every possible combination of the three possible combinations of spatial gradients in juvenile mortality, adult mortality, and recruitment, each with or without temporal variability, and with or without spatial variation in growth (Supplementary material Appendix 5 for the full list of models). We used the deviance information criterion (DIC), a Bayesian analogue to the Akaike information criteria (Spiegelhalter et al. 2002), to select the model that produced the most parsimonious fit to the data.

Field data for model validation

Larval recruitment

In August of 2002, we monitored oyster recruitment by deploying seven (15 × 15 cm) PVC tiles at five-meter intervals along an intertidal transect at sites E4 and W4. These tiles were removed after one month and oyster settlement to tiles was counted in the laboratory. We used the same procedure to monitor recruitment at all sites from 2003 to 2008 (Table 1), though the level of within-year and within-site replication varied adaptively depending on the magnitude of recruitment events (Supplementary material Appendix 6). During a prolonged recruitment drought (2003–2006), we increased our sampling within each year (more months) and within each site (more sampling units). Once recruitment resumed (2007–2008), we scaled back our sampling intensity within each year and site. Recruitment data were averaged to produce an annual site mean that was not biased by differences in sampling effort among years (Supplementary material Appendix 6). These empirical data provided annual patterns in oyster recruitment throughout the bay and were compared to model predictions; these empirical data were not used directly in the model.

Post-settlement oyster mortality

We estimated spatiotemporal patterns of recruitment in our model and tested these estimates with empirical observations. One concern about our interpretation of the estimated spatiotemporal patterns of recruitment was that the model was fit to survey patterns collected in the spring of each year, ~9 months after new larvae would have settled to the benthos. Thus the 'recruitment' pattern estimated by the model could reflect patterns of post-settlement mortality rather than patterns of physically-forced larval delivery. To distinguish between these alternatives, we performed a field experiment that estimated spatial variation of post-settlement oyster mortality due to predation and the environment. Strong spatial patterns of juvenile mortality would then inform our interpretation of the spatial recruitment patterns estimated by the model.

We took a standard cage/control outplant approach to quantify juvenile oyster mortality. In the summer of 2011, laboratory-reared larval oysters were allowed to settle onto sanded PVC tiles (0.10 × 0.10 m). Before deployment, juvenile oyster density was standardized to 20 oysters/tile and tiles were randomly assigned to receive one of three treatments: cage, cage-control and control. All cages were constructed using cylindrical galvanized metal frames that had 5 × 5 cm frame openings and a volume of 6635 cm^3. We wrapped the top, bottom and sides of each cage in clear plastic 0.3 cm mesh to exclude predators. To create the cage control, two openings (15 × 15 cm) were cut out of a cage's opposing sides (this allowed predator access, but preserved any artifactual effects of the cage itself on oyster mortality). We deployed 12 tiles (n = 4 per treatment) at sites E1, W2, W3, W4, and also at three sites between W3 and W4.

Before proceeding with our main analysis, we tested for procedural artifacts of the cages themselves. To perform this preliminary analysis, we focused on the cage and cage-control treatments only and used a generalized linear model (GLM, with binomial error and logit link, i.e. logistic regression) with oyster mortality after one month as the response variable and the factors 'treatment' (levels = control or cage-control), 'site' (categorical), and their interaction. A procedural artifact of the caging material was identified if either the term for treatment or the treatment × site interaction was statistically significant ($p < 0.05$). Given a significant interaction of treatment and site, we conducted a Tukey's post hoc test of cage-control and control means within each site. If a significant mean comparison occurred within a site, then that site was excluded from our main analysis. This procedure caused us to exclude three sites at which caging artifacts were detected (sites E1, W4, and one of the sites between W3 and W4).

We then proceeded with our main analysis, using a GLM (again with binomial error and logit link) to test whether oyster mortality after one month depended on treatment (cage versus control; cage-control treatments were excluded from this analysis), distance (km) from the ocean (to correspond to the distance effects in the population model), or an

interaction between treatment and distance. We used Tukey's post hoc test to compare means if main effects were statistically significant.

Data deposition

Data available from the Dryad Digital Repository: <http://dx.doi.org/10.5061/dryad.7jf0vp5> (Kimbro et al. 2018).

Results

Field data for model parameterization and fitting

Adult size and abundance surveys

Spatial trends of oyster abundance and size within Tomales Bay varied over time during this study. Oyster density increased with distance from the ocean in 2004, had no significant trend in 2005–2006, and peaked at an intermediate distance from the ocean in 2009 (Fig. 1B). By contrast, oyster length decreased with distance from the ocean in 2004, 2006 and 2009, and peaked at an intermediate distance in 2005 (Fig. 1C). These empirical survey data were used to fit the model.

Site-specific growth trajectories of oysters

In the 30-month outplant experiment, the growth trajectories of oysters (von Bertalanffy growth curve) displayed spatial variation that mirrored the spatial variation of phytoplankton abundance (bottom–up control, Fig. 1A) in Tomales Bay (Supplementary material Appendix 3 Fig. A3 for specific methods and results). These empirical growth data were used to parameterize the model.

State–space population model

Model selection identified one model that provided a substantially more parsimonious description of oyster size structure and density than all others (DIC weight >99%; Supplementary material Appendix 5). This model had oyster growth varying among sites rather than averaged across sites. In the model, juvenile mortality was estimated to be constant over both space and time (indicated by horizontal gray line and shaded confidence region in Fig. 2C). Meanwhile, adult mortality was estimated to be constant over time but bimodal in space, with the highest mortality in the inner bay, lowest in the mid-bay, and slightly higher towards the outer bay (indicated by the blue curve and shaded confidence region in Fig. 2C). In the model, recruitment also varied over time, and during years of high recruitment, followed a nonlinear, exponential gradient with a peak in the inner bay (curves and confidence regions shaded according to year in Fig. 2D). This most parsimonious model fit the size–abundance data at each site particularly well (Fig. 2A–B, Supplementary material Appendix 5), capturing spatial and interannual shifts in the abundance and size distribution at each site. For example, in 2006, mid-bay site W3 had much greater density of oysters but a size distribution shifted towards smaller sizes relative to outer-bay site E1 (Fig. 2A–B). The remaining models all had much worse performance ($\Delta DIC \geq 100$, $w < 1 \times 10^{-29}$) so we focused our analysis exclusively on the best model.

In examining the posterior distributions of recruitment and mortality rates obtained from the model, we focused our interpretation on values from 2004 and later because the initial model years represent transient behavior based on arbitrary starting conditions and because the first comparison to data occurs for the 2004 survey data. Because the model estimates of mortality integrated across all sources of mortality throughout the year, we did not attempt to compare their magnitude directly to mortality estimates derived only from short-term experiments during summer months. Nonetheless, the finding that juvenile mortality does not vary over space agrees with the 2011 experimental results.

The estimates for spatiotemporal patterns of recruitment from the best model afforded a good match to independent field estimates of recruitment collected over the same time period, which we present together in Fig. 2D. As with the mortality data, it is not appropriate to directly compare the magnitude of model and field estimates, because the model was fit to survey data collected in the spring, ~9 months after the summer/fall recruitment pulse when recruitment data were collected. Consequently, the model cannot separately estimate recruitment and post-recruitment/pre-census mortality, and so the magnitudes of model-estimated recruitment were considerably lower than the field estimates. Hence, the model outputs [curves and shaded confidence regions in Fig. 2D] are presented on a separate axis from the field data (points and error bars in Fig. 2D). Nonetheless, the model estimated near-zero recruitment for 2003–2006, which matched empirical estimates. No recruits were observed at the study sites in 2003–2005, and very few in 2006 (mean <1.5 recruit 0.01 m^2). In 2007 and 2008, the model matched the observed pattern of increasing recruitment towards the inner bay, with greater recruitment at all sites in 2008 than in 2007.

Field data for model validation: post-settlement oyster mortality experiment

In the 2011 post-settlement mortality experiment, oyster mortality inside of cages was high (~50%). Predators increased the mortality of juvenile oysters outside of cages further by 10% ($p < 0.001$, Fig. 3A, Supplementary material Appendix 7). These treatment differences were not influenced by an interaction with distance from the ocean ($p = 0.50$, Supplementary material Appendix 7). Given the lack of treatment × distance interaction, we examined the overall effect of distance on mortality in both treatments. Total mortality (predation + environment) increased slightly (<10%) with distance from the ocean ($p < 0.05$, Fig. 3B, Supplementary material Appendix 7). These results suggest that there was little spatial variation in predation and that the

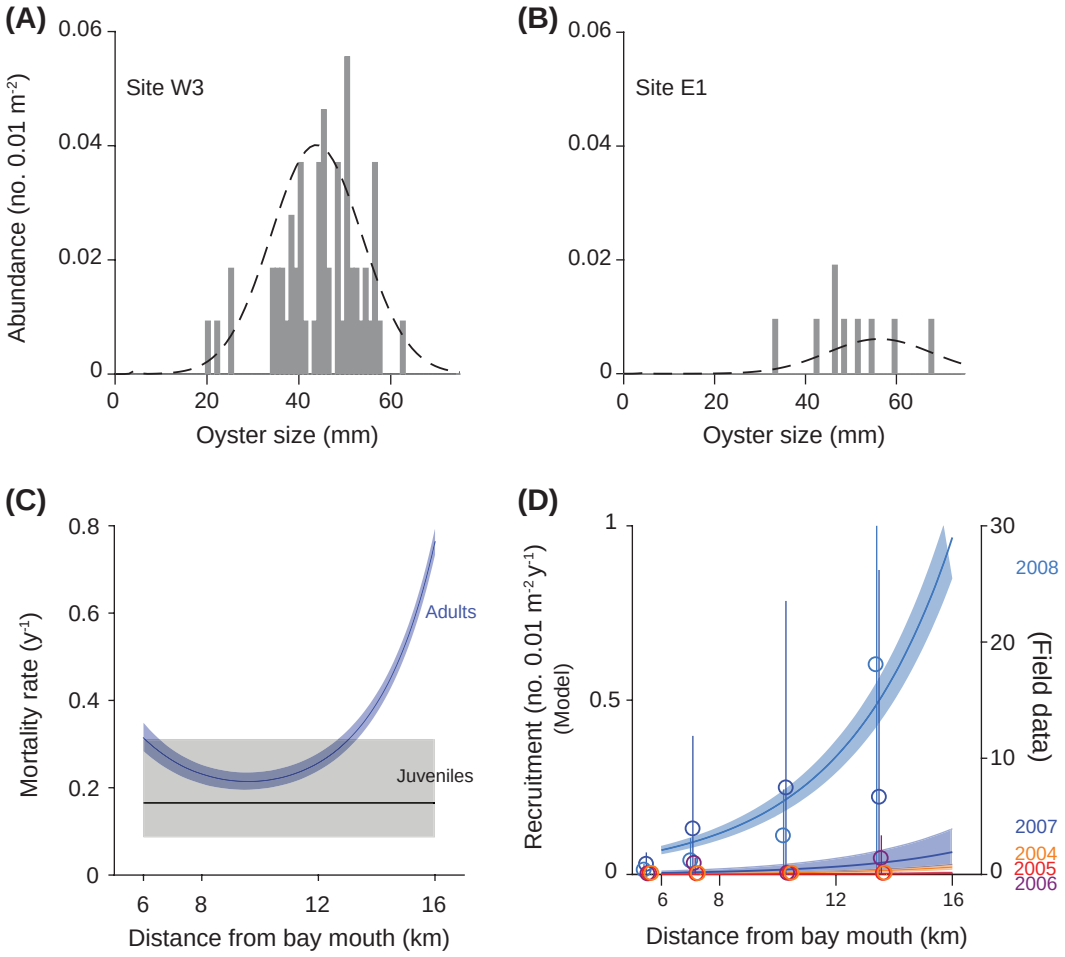

Figure 2. Summary of state–space model fitting. (A, B) Example fits of the model (curves) to observed size distributions (bars) in 2006 for sites W3 and E1. (C) Posterior estimates of juvenile (gray) and adult (blue) mortality rates as a function of distance from the mouth of Tomales Bay. (D) Posterior estimates of larval recruitment as a function of distance for years 2004–2009 (year indicated by color and text to the right of the axis). Field estimates of recruitment are also shown (open circles, values on right axis) as mean ± 95% confidence intervals. In (C, D), the solid line indicates the posterior mean, shading indicates the 50% credible interval.

majority of post-settlement mortality at all sites was caused by environmental factors.

Discussion

As is common in many systems, we found that a complex mixture of top–down, bottom–up and supply–side forces dictate variation in population dynamics of an important habitat-forming species. Our results derived from eight years of data collected through observations and experiments that identified potential controls of oyster growth, mortality and recruitment; all with potentially different gradients of variability over space and through time. By confronting these data with a suite of state–space models, we identified the most parsimonious combination of spatially- and temporally-explicit factors that influenced oyster population dynamics in a California estuary. Without this approach, we would have been limited to comparisons of statistically significant experimental results and field observations that were simply consistent with top–down versus bottom–up effects (Kos et al. 2011, Pierce et al. 2012). While field experimentation is powerful in its ability to isolate mechanisms and test hypotheses (Schmitt et al. 1999), reliance on experiments and surveys alone can be limited by a variety of factors. These include the scale or duration of experiments, over-reliance on statistical significance as a proxy for biological importance, and the inability to examine the simultaneous action of multiple factors. Therefore, the state–space modeling approach we have employed here demonstrates an important and powerful tool for disentangling complex causal processes in ecological systems (Hilborn and Mangel 1997).

Our focus on identifying the combination of processes shaping population distributions over space and time represents an important advance in quantifying the contributions of top–down, bottom–up and supply–side forces to interannual variation. This approach can be used to understand drivers of population dynamics in many other organisms with open

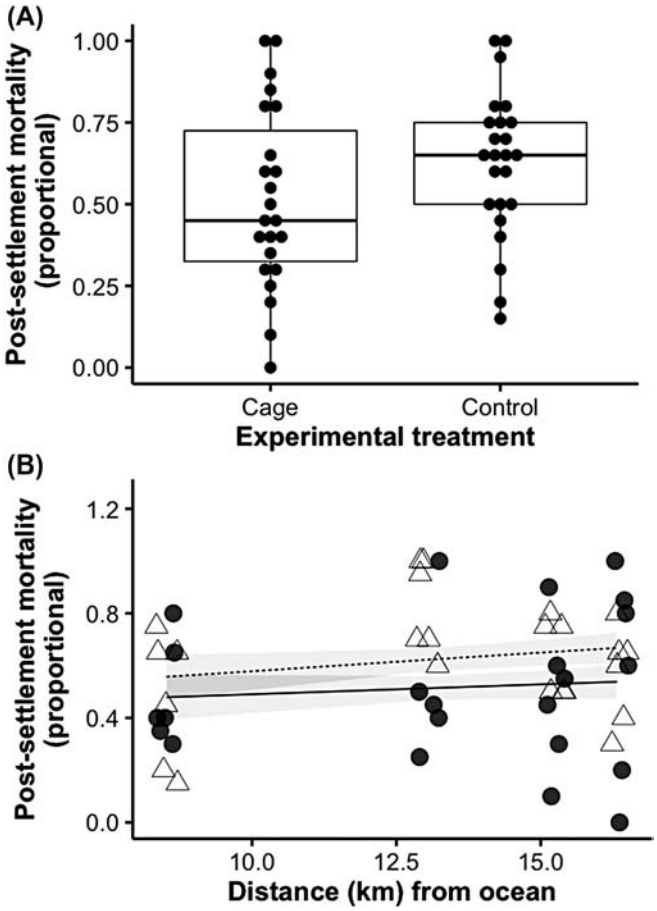

Figure 3. Post-settlement mortality of oysters in field experiment in 2011. (A) Mean (±SE) oyster mortality (proportional) in cage (predator exclusion) and control treatments. (B) Oyster mortality (proportional) as a function of distance from the ocean as well as cage (closed circles) and control (open triangles) treatments.

and/or physically-forced recruitment. In one example using an approach similar to ours, Johnson et al. (2012) applied model selection to identify explanatory statistical models for a long-time series of elk population surveys. For data that are more of a snapshot than a time series in nature, structural equation modeling coupled with model selection is a comparable solution for identifying top–down versus bottom–up controls, and it is growing in usage (Duffy et al. 2015, Menge et al. 2015).

We determined that the observed patterns of oyster population abundance and size structure were best explained by (a) spatiotemporal variation in oyster recruitment, (b) spatial variation in oyster growth and adult oyster mortality due to predation, but not (c) variation in juvenile oyster mortality. We are confident in the model's performance because these model results approximately matched the spatiotemporal patterns of independent experimental estimates of oyster vital rates and provided close fits to data. We used the model output to extrapolate possible drivers of variation in oyster demography. Specifically, we learned that spatiotemporal variation in size and abundance is set by a combination of environmentally-forced pulses of larval recruitment (supply–side) and a spatial gradient in adult mortality set by predator abundance (top–down). The latter is likely modulated by a matching gradient in growth patterns due to a bottom–up control of phytoplankton density. These insights surpass what we had learned from previous experiments and observations alone (Kimbro et al. 2009a, b). For example, while it had not been logistically feasible to replicate the adult mortality experiment (Kimbro et al. 2009a) over multiple years to test for temporal variability in predation, the model results suggest that any such temporal variation was not ecologically meaningful. Additionally, one would have expected juvenile mortality to follow a similar pattern as adult mortality, given the greater vulnerability of smaller oysters to all of the same predators that attack adult oysters. Surprisingly, this was not the case and we found that spatiotemporal differences in juvenile mortality were unimportant to overall patterns of abundance, relative to the effects of recruitment, growth and adult mortality.

Spatiotemporal patterns of oyster demography in Tomales Bay

The model results largely matched the spatiotemporal patterns of available independent estimates of oyster demographic rates, validating our results. With respect to bay-wide annual recruitment, model predictions agreed with average recruit densities across the bay (in years data were collected), including three years of recruitment failure in 2003–2005, very low recruitment in 2006, and then high recruitment in 2007–2008 (Fig. 2D). The model also matched the empirical pattern of increasing recruitment towards the inner bay in high recruitment years, particularly 2008. The agreement between empirical and model estimates was best for recruitment preceding years in which survey data were available, because only in those years did the model recruitment estimate directly affect the likelihood calculation. Hence the model–data correspondence was better in 2008 (when fall recruitment preceded the 2009 survey) than in 2007, in which the model slightly underestimated actual recruitment.

Based on our knowledge of Tomales Bay, we can offer explanations for the sources of variability in recruitment revealed by our model. The Olympia oyster has a relatively short pelagic larval duration of 28–42 d (Baker 1995, Pritchard et al. 2015). Given the mean residence time of 60 d in Tomales Bay and >100 d in the inner bay (Hearn and Largier 1997) as well as the distance to the nearest other substantial oyster population (San Francisco Bay, >60 km), it is likely that most larval recruits are locally produced. Thus, inter-annual variability in recruitment could reflect variation in spawning success or larval mortality within and near the bay, both of which are likely related to the timing and magnitude of planktonic productivity during the reproductive season. The pattern of recruitment density increasing with greater distance from the bay mouth (Fig. 2D) likely reflects

the longer residence times in the inner bay (Hearn and Largier 1997, Largier et al. 1997). Longer residence times allow more larvae to complete development and settle within the bay rather than being flushed out prior to settlement.

We should caution that the 'recruitment' term in the model describes the appearance of new individuals in the survey data in the spring of a given year. However, those new recruits would have actually settled to the benthos the previous autumn. Consequently, it is possible that the spatiotemporal patterns of recruitment in the model reflect post-settlement factors rather than larval processes. However, the lack of substantial spatial variation in the empirical estimates of post-settlement mortality (Fig. 3B) suggests that spatial patterns of recruitment were indeed set at the time of settlement by physical forcing (water residence time).

The best model contained spatial structure in the growth trajectories of oysters. Analysis by Kimbro et al. (2009b) revealed that this spatial variability was caused by patterns of phytoplankton biomass within the bay. The combination of moderate residence time and nutrient concentrations in the mid-bay led to higher phytoplankton biomass and thus faster oyster growth. The spatial differences in growth were manifest most prominently as differences in the asymptotic maximum size (Supplementary material Appendix 3) in the adult stage, which was also the stage in which there are spatial differences in mortality rates. As we explain in the next paragraph, we believe those patterns are linked. Our model did not consider temporal variation in growth, because prior experiments showed that the spatial pattern of growth rates across the bay was consistent across two years (Kimbro et al. 2009b).

Model-predicted mortality rates were more difficult to compare to empirical estimates because we only quantified mortality directly in 2005–2006 and 2011, and because the model integrates mortality across the entire year rather than over shorter experimental time scales. However, the available comparisons support the model. Kimbro et al. (2009a) found that adult oyster mortality was lowest in the mid-bay, and higher at inner bay and outer bay sites, similar to the pattern estimated by the model (Fig. 2C). This pattern could, in part, be attributed to the growth patterns driven by bottom–up forcing: oysters grow faster in the mid-bay, so they may be able to enter more quickly into a size refuge from native snails, which appear to prefer smaller prey such as barnacles and juvenile oysters (Baker 1995, Kimbro and Grosholz unpubl.).

The spatial pattern of adult oyster mortality identified by the model also corresponds with the spatial pattern of predator abundance in the bay, with higher densities of native predators in the outer and middle bay regions (excluding invasive predators), and the more low-salinity-tolerant invasive predators in the inner bay (Kimbro et al. 2009a, Cheng and Grosholz 2016). The invasive whelks in the inner bay exert higher predation mortality on oysters than do the native whelks in the middle and outer bays apparently because of a trait-mediated indirect interaction (TMII); the native whelk forages less in the presence of its native crab predator, while the invasive whelk does not have the same response to the native or invasive crab (Kimbro et al. 2009a).

The lack of spatial variation in juvenile oyster mortality estimated by the model was somewhat surprising, though it does agree with the 2011 experimental results. Despite the potential for spatial variation in predation on juvenile oysters (i.e. high in inner bay and low elsewhere, as we detected in the adult oysters), there does not seem to be any such variation. Based on our 2011 field experiment and more recent laboratory experiments (Bible et al. 2017), we speculate that juvenile mortality is spatially homogeneous because most juvenile oysters die from exposure to multiple environmental factors (such as desiccation during low tide and salinity fluctuations) before predators can exert strong top–down control. Hence spatial variation in predation does not become an important factor until later in life.

The lack of spatiotemporal variation in juvenile mortality implies an absence of density-dependence in the juvenile stage. This would have been reflected in higher mortality in the inner bay during high-recruitment years. This is a contrast to the dynamics of many other demographically open coastal marine populations, in which the spatiotemporal variability in recruitment is tempered by density-dependent juvenile mortality (e.g. coral reef fishes; Caselle and Warner 1996, White and Warner 2007); which itself often varies in strength over space and time (White 2007). Again, the only apparent explanation for this difference is that most juvenile Olympia oyster mortality is due to density-independent environmental stressors, as has been consistently found in eastern oysters *Crassostrea virginica* as well (Shumway 1996).

Conclusions

It has become clichéd to point out that no single ecological paradigm (top–down/bottom–up) is at work in a given study system (Menge 1992, Power 1992). Now, the challenge is to follow such a statement with insight into where, when, and how different processes operate and their relative importance. We addressed this challenge by using an approach that quantified the variability in multiple processes, rather than simply testing single factors, for example, examining mortality or grazing rates at different sites (Leonard et al. 1998, Menge et al. 2003, Orrock et al. 2014). Looking forward, a more powerful approach to ecological inferences would be to couple mechanistic modeling of observational data with targeted experiments (e.g. predator exclosures) during the same time period in order to test the model inferences rigorously, thus uniting the CEA and state–space techniques.

Acknowledgements – We thank S. Attoe, A. Baukus, L. Budd, A. Chang, B. Cheng, C. Coleman-Hurlbert, A. Deck, M. Ferner, M. O'Leary, B. Steves and C. Zabin for assistance with monitoring and experiments. We particularly thank B. Cheng for leading the implementation and data collection of 2011 field experiment and

A. Deck for collecting the recruitment data in 2008. This manuscript was improved by conversations with L. Botsford, A. R. Hughes, B. Jaffee, J. Largier, M. O'Farrell and J. Stachowicz, and by helpful comments from S. Navarrete. This article is dedicated to the memory of Dr. Susan L. Williams, who inspired our science and humanity.

Funding – This research was supported by funding from the Pacific Coast Science and Learning Center at the Point Reyes National Seashore (to DLK), the University of California Marine Council/Coastal Environmental Quality Initiative (to DLK), UC Davis Graduate Group in Ecology (to DLK), the Bodega Marine Laboratory (to DLK), the National Science Foundation (awards OCE-1736943 to DLK, OCE-1514893 to EDG, and OCE-1435473 to JWW), National Oceanographic and Oceanic Administration – National Estuarine Research Reserve Science Collaborative (to EDG), California Sea Grant (to EDG), California Ocean Protection Council (to EDG), University of California EIPD program (to EDG), National Park Service Cooperative Ecosystem Studies program and Pacific States Marine Fisheries Commission (to EDG). This is contribution 382 from the Northeastern University Marine Science Center in Nahant and 487 from PISCO, the Partnership for Interdisciplinary Study of Coastal Oceans.

Author contributions – DLK and JWW contributed equally to this paper. All authors conceived idea for the study. DLK and EDG designed and conducted the experiments and surveys; JWW statistically analysed the majority of the data and conducted the modelling; DLK and JWW wrote the first draft of the paper and EDG made significant contributions to all subsequent drafts.

References

Baker, P. 1995. Review of ecology and fishery of the Olympia oyster, *Ostrea lurida* with annotated bibliography. – J. Shellfish Res. 14: 501–518.

Bible, J. M. et al. 2017. Timing of stressors alters interactive effects on a coastal foundation species. – Ecology 98: 2468–2478.

Botsford, L. W. et al. 1994. Bimodality in size distributions: the Red Sea urchin *Strongylocentrotus franciscanus* as an example. – Ecol. Appl. 4: 42–50.

Carpenter et al. 1985. Cascading trophic interactions and lake productivity. – BioScience 35: 634–639.

Caselle, J. E. and Warner, R. R. 1996. Variability in recruitment of coral reef fishes: the importance of habitat at two spatial scales. – Ecology 77: 2488–2504.

Caswell, H. 2001. Matrix population models. – Sinauer Assoc., MA.

Cheng, B. S. and Grosholz, E. D. 2016. Environmental stress mediates trophic cascade strength and resistance to invasion. – Ecosphere 7: e01247.10.1002/ecs2.1247

Cheng, B. S. et al. 2017. Trophic sensitivity of invasive predator and native prey interactions: integrating environmental context and climate change. – Funct. Ecol. 31: 642–652.

de Valpine, P. and Hastings, A. 2002. Fitting population models incorporating process noise and observation error. – Ecol. Monogr. 72: 57–76.

Dennis, B. et al. 2006. Estimating density-dependence, process noise and observation error. – Ecol. Monogr. 76: 232–341

Duffy, J. E. et al. 2015. Biodiversity mediates top–down control in eelgrass ecosystems: a global comparative-experimental approach. – Ecol. Lett. 18: 696–705.

Easterling, M. R. et al. 2000. Size-specific sensitivity: applying a new structured population model. – Ecology 81: 694–708.

Ellner, S. P. et al. 2016. Data-driven modelling of structured populations. – Springer.

Elmhagen, B. and Rushton, S. P. 2007. Trophic control of mesopredators in terrestrial ecosystems: top–down or bottom–up? – Ecol. Lett. 10: 197–206.

Gaines, S. and Roughgarden, J. 1985. Larval settlement rate: a leading determinant of structure in an ecological community of the marine intertidal zone. – Proc. Natl Acad. Sci. USA 82: 3707–3711.

Hairston, N. G. et al. 1960. Community structure, population control, and competition. – Am. Nat. 94: 421–425.

Hastings, A. 2010. Timescales, dynamics, and ecological understanding. – Ecology 91: 3471–3480.

Hearn, C. J. and Largier, J. L. 1997. The summer buoyancy dynamics of a shallow Mediterranean estuary and some effects of changing bathymetry: Tomales Bay, California. – Estuar. Coast. Shelf Sci. 45: 497–506.

Hilborn, R. and Mangel, M. 1997. The ecological detective: confronting models with data. – Princeton Univ. Press.

Jensen, G. C. et al. 2007. Biotic resistance to green crab, *Carcinus maenas*, in California bays. – Mar. Biol. 151: 2231–2243.

Johnson, B. K. et al. 2012. Abiotic, bottom–up, and top–down influences on recruitment of Rocky Mountain elk in Oregon: a retrospective analysis. – J. Wildl Manage. 77: 102–116.

Kalman, R. E. 1960. A new approach to linear filtering and prediction problems. – Trans. ASME J. Basic Eng. D 82: 35–45

Kimbro, D. L. and Grosholz, E. D. 2006. Disturbance influences oyster community richness and evenness, but not diversity. – Ecology 87: 2378–2388.

Kimbro, D. L. et al. 2009a. Invasive species cause large-scale loss of native California oyster habitat by disrupting trophic cascades. – Oecologia 160: 563–575.

Kimbro, D. L. et al. 2009b. Coastal oceanographic processes influence the growth and size of a key estuarine species, the Olympia oyster. – Limnol. Oceanogr. 54: 1425–1437.

Kimbro, D. L. et al. 2018. Data from: the dynamics of open populations: integration of top–down, bottom–up and supply–side influences on intertidal oysters. – Dryad Digital Repository, <http://dx.doi.org/10.5061/dryad.7jf0vp5>.

Knape, J. and de Valpine, P. 2012. Fitting complex population models by combining particle filters with Markov chain Monte Carlo. – Ecology 93: 256–263.

Kos, M. et al. 2011. Relative importance of plant-mediated bottom–up and top–down forces on herbivore abundance on *Brassica oleracea*. – Funct. Ecol. 25: 1113–1124.

Largier, J. L. et al. 1997. Seasonally hypersaline estuaries in Mediterranean-climate regions. – Estuar. Coast. Shelf Sci. 45: 789–797.

Leonard, G. H. et al. 1998. Flow-driven variation in intertidal community structure in a Maine estuary. – Ecology 79: 1395–1411.

Lewin, R. 1986. Supply–side ecology: existing models of population structure and dynamics of ecological communities have tended to ignore the effect of the influx of new members into the communities. – Science 234: 25–27.

Menge, B. 2000. Top–down and bottom–up community regulation in marine rocky intertidal habitats. – J. Exp. Mar. Biol. Ecol. 250: 257–289.

Menge, B. A. 1992. Community regulation – under what conditions are bottom–up factors important on rocky shores. – Ecology 73: 755–765.
Menge, B. A. et al. 2003. Coastal oceanography sets the pace of rocky intertidal community dynamics. – Proc. Natl Acad. Sci. USA 100: 12229–12234.
Menge, B. A. et al. 2015. Are meta-ecosystems organized hierarchically? A model and test in rocky intertidal habitats. – Ecol. Monogr. 85: 213–233.
Orrock, J. L. et al. 2014. A continent-wide study reveals clear relationships between regional abiotic conditions and post-dispersal seed predation. – J. Biogeogr. 42: 662–670.
Patterson, T. A. et al. 2008. State–space models of individual animal movement. – Trends Ecol. Evol. 23: 87–94
Pierce, B. M. et al. 2012. 2012. Top–down versus bottom–up forcing: evidence from mountain lions and mule deer. – J. Mammal. 93: 977–988.
Polis, G. A. and Hurd, S. 1996. Linking marine and terrestrial food webs: allochthonous input from the ocean supports high secondary productivity on small islands and coastal land communities. – Am. Nat. 147: 396–423.
Polishchuk, L. V. et al. 2012. How to measure top–down versus bottom–up effects: a new population metric and its calibration on *Daphnia*. – Oikos 122: 1177–1186.
Power, M. E. 1992. Top–down and bottom–up forces in food webs: do plants have primacy. – Ecology 73: 733–746.
Pritchard, C. et al. 2015. The Olympia oyster *Ostrea lurida*: recent advances in natural history, ecology and restoration. – J. Shellfish Res. 34: 259–271.
Schmitt, R. J. et al. 1999. Quantifying the effects of multiple processes on local abundance: a cohort approach for open populations. – Ecol. Lett. 2: 294–303.
Shumway, S. E. 1996 Natural environmental factors. – In: Kennedy, V. S. et al. (eds.), The eastern oyster, *Crassostrea virginica*. – Maryland Sea Grant, pp. 467–513.
Spiegelhalter, D. J. et al. 2002. Bayesian measures of model complexity and fit. – J. R. Stat. Soc. B 64: 583–639.
Stiling, P. and Rossi, A. M. 1997. Experimental manipulation of top–down and bottom–up factors in a tri-trophic system. – Ecology 78: 1602–1606.
Tegner, M. J. and Dayton, P. K. 1981. Population structure, recruitment and mortality of two sea urchins (*Strongylocentrotus franciscanus* and *S. purpuratus*) in a kelp forest. – Mar. Ecol. Prog. Ser. 5: 255–268.
Tegner, M. J. and Levin, L. A. 1983. Spiny lobsters and sea urchins: analysis of a predator–prey interaction. – J. Exp. Mar. Biol. Ecol. 73: 125–150.
White, J. W. 2007. Spatially correlated recruitment of a marine predator and its prey shapes the large-scale pattern of density-dependent prey mortality. – Ecol. Lett. 10: 1054–1065.
White, J. W. and Warner, R. R. 2007. Safety in numbers and the spatial scaling of density-dependent mortality in a coral reef fish. – Ecology 88: 3044–3054.
White, J. W. et al. 2016. Fitting state–space integral projection models to size-structured time series data to estimate unknown parameters. – Ecol. Appl. 26: 2677–2694.
Wing, S. R. et al. 1998. Meroplanktonic distribution and circulation in a coastal retention zone of the northern California upwelling system. – Limnol. Oceanogr. 43: 1710–1721.

Supplementary material (available online as Appendix oik-05892 at <www.oikosjournal.org/appendix/oik-05892>). Appendix 1–7.